

# On the Flux and Photon Index Distributions of Fermi-LAT Blazars

J. Singal, V. Petrosian, M. Ajello

Stanford / KIPAC / SLAC

We present a determination of the distributions of gamma-ray flux and photon index for the 352 blazars detected at greater than  $7\sigma$  and above  $\pm 20^\circ$  Galactic latitude by the Fermi-LAT in its first year catalog. Our method reconstructs the intrinsic distributions from the observed ones in a way that accounts robustly for the selection biases in the data and correlations among the variables. We find that for the population as a whole the intrinsic flux distribution can be represented by a broken power law of slopes  $-2.37 \pm 0.13$  and  $-1.70 \pm 0.26$ , and the intrinsic photon index distribution can be represented by a Gaussian with mean  $2.41 \pm 0.13$  and  $1\sigma$  width of  $0.25 \pm 0.03$ . We also find the intrinsic distributions for the sub populations of BL Lac and FSRQ type blazars considered separately.

## Fermi-LAT Blazars

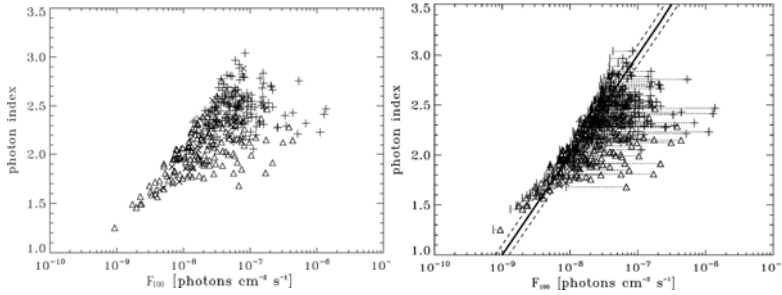


Figure 1: Left: Flux and photon index for the 352 Fermi blazars used in this analysis. BL Lac type blazars ( $n=163$ ) are shown as triangles, FSRQ type blazars ( $n=161$ ) are shown as vertical crosses, and blazars of unidentified or ambiguous type ( $n=28$ ) are represented by Xs. Right: Same, but with the cutoff function shown, along with the approximate limiting flux for each object determined by the detection significance.

We use blazars from the first year Fermi-LAT extragalactic catalog.<sup>2</sup> Fermi-LAT observations are biased against soft spectrum blazar sources at fluxes below  $F_{100} \approx 10^{-7}$  photons  $\text{cm}^{-2}$   $\text{sec}^{-1}$ . Because of this truncation in the data, and because of the possible inherent correlation between photon index ( $\Gamma$ ) and flux ( $F_{100}$ ), accessing the true distributions of photon index and flux requires care.

## Methods

First we determine the correlation between  $\alpha$  and  $F_{100}$  using the Spearman rank test (SRT) with the method of associated sets,<sup>3,4</sup> which can deal with truncated data. We approximate the cutoff function with a curve in the  $\Gamma, F_{100}$  plane as discussed in [1]. We then can take out the correlation to form a correlation reduced photon index:

$$\Gamma_{cr} = \Gamma - \beta \cdot \text{Log} \left( \frac{F_{100}}{F_{100-\text{min}}} \right) \quad (1)$$

where  $\beta$  is the best fit correlation parameter. Then the distributions are separable:

$$G(F_{100}, \Gamma) = \psi(F_{100}) \times \hat{h}(\Gamma) \quad (2)$$

and the intrinsic photon index distribution can be recovered by

$$h(\Gamma) = \int_{F_{100}} \psi(F_{100}) \hat{h} \left( \Gamma - \beta \cdot \text{Log} \left( \frac{F_{100}}{F_{100-\text{min}}} \right) \right) dF_{100} \quad (3)$$

## Distributions

We form the distributions  $\psi(F_{100})$  and  $\hat{h}(\Gamma)$  using the Lynden-Bell method modified with associated sets<sup>3,4</sup> to account for the truncation in the  $\Gamma, F_{100}$  plane. A full discussion is provided in [1].

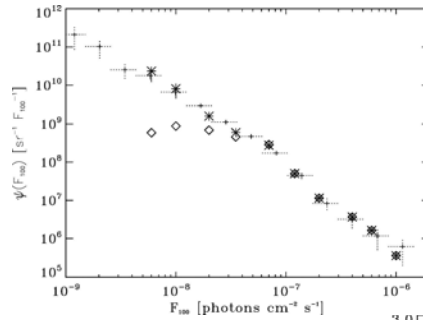


Figure 2: Observed (diamonds) and reconstructed intrinsic (stars) distribution of flux  $\psi(F_{100})$  for the 352 Fermi blazars used in this analysis. We also plot  $\psi(F_{100})$  as determined in MA<sup>5</sup> (small crosses), with error bars (dotted lines).

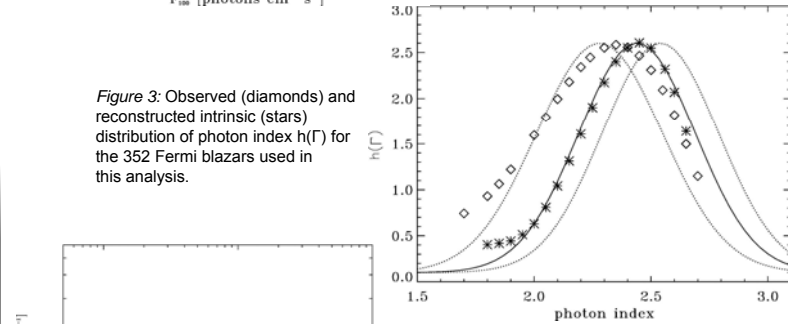
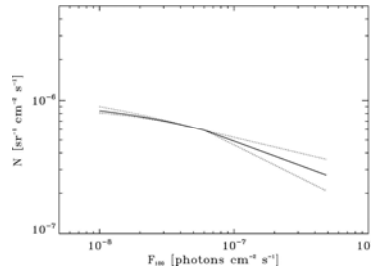


Figure 3: Observed (diamonds) and reconstructed intrinsic (stars) distribution of photon index  $h(\Gamma)$  for the 352 Fermi blazars used in this analysis.

Figure 4: Estimate of the total cumulative photon density from the Fermi blazars, The diffuse gamma-ray background would correspond to  $\sim 1 \times 10^{-5}$  MeV  $\text{cm}^{-2}$   $\text{sec}^{-1}$   $\text{sr}^{-1}$  in these units.<sup>6</sup>



	$n$	$\beta^a$	$m_{\text{above}}^b$	$F_{\text{break}}^c$	$m_{\text{below}}^d$	$\mu^e$	$\sigma^f$
Blazars <sup>g</sup> (this work)	352	$0.02 \pm 0.08$	$-2.37 \pm 0.13$	6.0	$-1.70 \pm 0.26$	$2.41 \pm 0.13$	$0.25 \pm 0.03$
Blazars <sup>g</sup> (MA) <sup>5</sup>	352	-	$-2.48 \pm 0.13$	$7.39 \pm 1.01$	$-1.57 \pm 0.09$	$2.37 \pm 0.02$	$0.28 \pm 0.01$
BL Lacs (this work)	163	$0.04 \pm 0.09$	$-2.55 \pm 0.17$	5.5	$-1.61 \pm 0.27$	$2.13 \pm 0.13$	$0.24 \pm 0.02$
BL Lacs (MA) <sup>5</sup>	163	-	$-2.74 \pm 0.30$	$6.77 \pm 1.30$	$-1.72 \pm 0.14$	$2.18 \pm 0.02$	$0.23 \pm 0.01$
FSRQs (this work)	161	$-0.11 \pm 0.06$	$-2.22 \pm 0.09$	6.0	$-1.62 \pm 0.55$	$2.52 \pm 0.08$	$0.17 \pm 0.02$
FSRQs (MA) <sup>5</sup>	161	-	$-2.41 \pm 0.16$	$6.12 \pm 1.30$	$-0.70 \pm 0.30$	$2.48 \pm 0.02$	$0.18 \pm 0.01$

<sup>a</sup> The correlation between photon index  $\Gamma$  and flux  $F_{100}$ . See Equation 1 and §3.1.

<sup>b</sup> The slope of the intrinsic flux distribution  $\psi(F_{100})$  at fluxes above the break.

<sup>c</sup> The flux at which the power law break in  $\psi(F_{100})$  occurs, in units of  $10^{-8}$  photons  $\text{cm}^{-2}$   $\text{sec}^{-1}$ . In MA this is a fit, while in this work it is a visual inspection, as precise location of the break is not important for this analysis.

<sup>d</sup> The slope of the intrinsic flux distribution  $\psi(F_{100})$  at fluxes below the break.

<sup>e</sup> The mean of the Gaussian fit to the intrinsic photon index distribution  $h(\Gamma)$ . For the analysis here this includes the full range of results and their uncertainties when considering the  $1\sigma$  range of  $\beta$ .

<sup>f</sup> The  $1\sigma$  width of the Gaussian fit to the intrinsic photon index distribution  $h(\Gamma)$ .

<sup>g</sup> Including all FSRQs, BL Lacs, and 28 of unidentified type.